

Conformal Field Theory Ground States as Critical Points of an Entropy Function

Ting-Chun Lin (林鼎鈞)^{1,2} and John McGreevy¹

¹*Department of Physics, University of California at San Diego, La Jolla, CA 92093, USA*

²*Hon Hai Research Institute, Taipei, Taiwan*

(Dated: March 10, 2023)

We derive an entropy formula satisfied by the ground states of 1+1D conformal field theories. The formula implies that the ground state is the critical point of an entropy function. We conjecture that this formula may serve as an information-theoretic criterion for conformal field theories, which differs from the conventional algebraic definition. In addition to these findings, we use the same proof method to extract the six global conformal generators of the conformal field theory from its ground state. We validate our results by testing them on different critical lattice models with excellent agreement.

Quantum entanglement and quantum information have played important roles in the study of quantum matter. For 2+1D gapped phases, this includes topological entanglement entropy [1, 2], entanglement spectrum [3], and the recent work on chiral central charge [4]. For 1+1D conformal field theories (CFTs), the entanglement entropy [5–7] of the ground state is related to the central charge. These tools are useful to distinguish quantum phases analytically and numerically.

More ambitiously, one may wonder if the reverse holds, namely, could there be entanglement conditions that are satisfied and only satisfied by ground states for certain quantum phases? One proposal is given by Shi, Kato, and Kim [8] where they stated two conditions that are conjectured to be satisfied and only satisfied by the ground states of topological quantum field theories¹. Remarkably, using the two conditions, they are able to derive many known properties of 2+1D topological orders. Another nice feature is that because the two conditions only involve the entropies of local regions, the conditions can be checked easily. This program is called entanglement bootstrap and can be applied to other settings, including gapped domain walls [9] and higher dimensions [10].

Given the success of entanglement bootstrap for gapped topological orders, one may wonder if a similar set of entropy conditions exists for gapless states. In this work, we propose a new set of ultra-violet (UV)-independent entropy conditions that apply to the ground states of 1+1D unitary CFTs. The conditions additionally hold for 1+1D gapped phases at RG fixed points. In the spirit of entanglement bootstrap, we conjecture that these conditions characterize the ground states of 1+1D RG fixed points with Lorentz symmetry.

Let A, B, C be three consecutive intervals; see Figure 1. The main result states that the ground state of a 1+1D

unitary CFT $|\psi\rangle$ satisfies

$$K_\Delta \propto I \quad \text{and} \quad K_\Delta |\psi\rangle \propto |\psi\rangle \quad (1)$$

where

$$K_\Delta := (K_{AB} + K_{BC}) - \eta(K_A + K_C) - (1 - \eta)(K_B + K_{ABC}) \quad (2)$$

and² $K_X := -\log \rho_X$ is the entanglement Hamiltonian of the reduced density matrix $\rho_X := \text{Tr}_{\bar{X}} |\psi\rangle\langle\psi|$, I is the identity operator, and η is the cross ratio of the intervals. Moreover, when the central charge c is known, the proportionality constant is given by

$$K_\Delta = \frac{c}{3} h(\eta) \quad \text{and} \quad K_\Delta |\psi\rangle = \frac{c}{3} h(\eta) |\psi\rangle \quad (3)$$

where $h(\eta) := -\eta \log \eta - (1 - \eta) \log(1 - \eta)$ is the binary entropy function. Finally, we observe that eq:main-eq is the condition for $|\psi\rangle$ to be a critical point of the following function:

$$S_\Delta(|\psi\rangle) := (S_{AB} + S_{BC}) - \eta(S_A + S_C) - (1 - \eta)(S_B + S_{ABC}) \quad (4)$$

where $S_X := S(\rho_X)$ is the von Neumann entanglement entropy between X and \bar{X} . The function is nonnegative because it is a convex combination of two nonnegative quantities, by weak monotonicity $S_{AB} + S_{BC} - S_A - S_C \geq 0$ and strong subadditivity $S_{AB} + S_{BC} - S_B - S_{ABC} \geq 0$ [11, 12]. All the statements above can be extended to the ground state on a finite circle and the thermal state on an infinite line. Importantly, even though the equations are derived for exact CFT ground states, we show numerically that the equations hold approximately for various

¹ More precisely, any state that satisfies the conditions is the ground state of a Hamiltonian that belongs to a topological phase. And any topological phase has a Hamiltonian whose ground state satisfies the conditions.

² The reader might worry that $-\log \rho_X$ is not well-defined when ρ_X has zero eigenvalues. Here, we note that the equation $K_\Delta |\psi\rangle \propto |\psi\rangle$ remains well-defined, because it projects out the problematic eigenvectors. This point is discussed in further detail after the derivation of the main results.

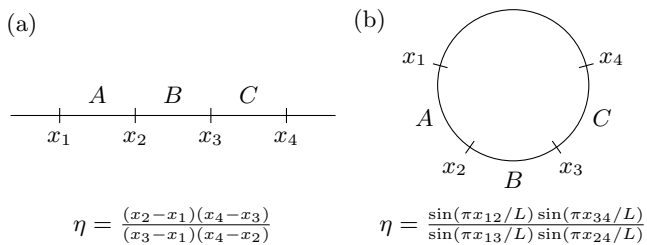


FIG. 1. (a) Three consecutive intervals on an infinite system with the corresponding cross ratio η . (b) Three consecutive intervals on a circle with circumference L . Here, $x_{ij} := x_j - x_i$ denotes the distance between x_i and x_j .

lattice models and the error $\left|K_{\Delta}|\psi\rangle - \frac{c}{3}h(\eta)|\psi\rangle\right|$ decays as the number of sites increases (as a power law).

After obtaining the basic formulas, we explore their implications on states supported on a discrete lattice. Our goal is to identify new equations that could potentially hold for lattice models, which can then be validated numerically. Specifically, we express the entanglement Hamiltonians of intervals and the six global conformal generators as a combination of 1-site and 2-site entanglement Hamiltonians of the CFT ground state. This has two important implications. First, when the state satisfies the entropy formula, the six global conformal generators have the expected scaling properties under real-space RG. This provides evidence that a state satisfying the entropy formula enjoys conformal symmetry. Second, the result yields an algorithm that can reconstruct the CFT local Hamiltonian from the CFT ground state. This is remarkable since the parent Hamiltonian construction [13] that applies to matrix product states cannot be applied to gapless phases due to their long-range correlations. This algorithm offers an alternative method for recovering the local Hamiltonians from states near RG fixed points, including gapped and gapless phases.

We want to highlight an implicit theme of this work, which aims to go beyond the traditional algebraic formulation of CFT and provide an alternative analytic formulation. Typically, CFTs are defined using algebras with equalities, which do not allow for the discussion of *approximate CFTs*. However, many examples exist that we would like to categorize as approximate CFTs, such as QFTs that are slight perturbations of CFTs or critical lattice models that are CFTs in the IR limit. Because these models have different Hilbert spaces, finding a criterion that applies to all cases is challenging. To address this issue, we utilize the entanglement entropy and entanglement Hamiltonian, which are agnostic to the Hilbert space. We propose to define approximate CFTs as systems whose ground state approximately satisfies Eq. 1. Further research is needed to determine the usefulness of this proposal.

CFTs and their entanglement properties— Conformal field theories (CFTs) are field theories with scale invariance. Such scale invariance often implies a larger invariance called the conformal symmetries, which include transformations that locally look like rescalings. These conformal symmetries appear naturally in many physical systems, including the fixed points of the RG flow and the critical points of statistical models.

For 1+1D CFT, the entanglement entropy [7] and the entanglement Hamiltonian (EH) [14] of the ground state on an interval $[x_1, x_2]$ are known to be

$$S_{[x_1, x_2]} = \frac{c}{3} \log \frac{x_2 - x_1}{\epsilon} \quad (5)$$

and

$$K_{[x_1, x_2]} = 2\pi \int_{x_1}^{x_2} dx \frac{(x - x_1)(x_2 - x)}{x_2 - x_1} T_{00}(x) + \text{const.} \quad (6)$$

where c is the central charge, ϵ is the uniform UV cutoff, T is the stress-energy tensor, and const. is a number that depends on the UV cutoff ϵ . These two equations are the key to showing the main results. As we will see, even though both equations suffer from UV divergences, the combinations in Eq. (1) and Eq. (3) are free from UV divergences.

Derivation of the main results— We first show Eq. (1) and Eq. (3) for the ground state of a 1+1D CFT on an infinite system. Then we show the equivalence of Eq. (1) to the critical point condition of S_{Δ} defined in Eq. (4). Let $A = [x_1, x_2]$, $B = [x_2, x_3]$, and $C = [x_3, x_4]$ be three consecutive intervals. For convenience, we define the function $f_{[x', x'']}(x) = \frac{(x-x')(x''-x)}{x''-x'} 1_{[x', x'']}$ where $1_{[x', x'']}$ is the indicator function. By Eq. (6),

$$\begin{aligned} & (K_{AB} + K_{BC}) - \eta(K_A + K_C) - (1 - \eta)(K_B + K_{ABC}) \\ &= \int_{-\infty}^{\infty} dx ((f_{AB} + f_{BC}) - \eta(f_A + f_C) \\ & \quad - (1 - \eta)(f_B + f_{ABC})) T_{00}(x) + \text{const.} \quad (7) \end{aligned}$$

A straightforward calculation shows $(f_{AB} + f_{BC}) - \eta(f_A + f_C) - (1 - \eta)(f_B + f_{ABC}) = 0$ from which Equation (1) follows.

To obtain the ratio in Eq. (3), we multiply $\langle\psi|$ on both sides. Because $\langle\psi|K_A|\psi\rangle = S_A$, the left hand side becomes $(S_{AB} + S_{BC}) - \eta(S_A + S_C) - (1 - \eta)(S_B + S_{ABC})$ which evaluates to $\frac{c}{3}h(\eta)$ using Eq. (5).

Now we show that Eq. (1) is precisely the condition for vanishing variation of S_{Δ} with respect to the state. Recall that $|\psi\rangle$ is a critical point if the gradient is 0 subject to $(\langle\psi| + \langle d\psi|)(|\psi\rangle + |d\psi\rangle) = 1$, i.e., $\langle d\psi|\psi\rangle + \langle\psi|d\psi\rangle = 0$. To compute the gradient of $S_{\Delta} = (S_{AB} + S_{BC}) - \eta(S_A + S_C) - (1 - \eta)(S_B + S_{ABC})$ we use the first order derivative of the entanglement entropy:

$$dS_X(|\psi\rangle) = \langle d\psi|K_X|\psi\rangle + \langle\psi|K_X|d\psi\rangle \quad (8)$$

as reviewed in the Supplementary Material. Therefore, the critical point $|\psi\rangle$ has

$$dS_\Delta = \langle d\psi|K_\Delta|\psi\rangle + \langle\psi|K_\Delta|d\psi\rangle = 0 \quad (9)$$

for all $|d\psi\rangle$ satisfying $\langle d\psi|\psi\rangle + \langle\psi|d\psi\rangle = 0$. Recall $K_\Delta = (K_{AB} + K_{BC}) - \eta(K_A + K_C) - (1 - \eta)(K_B + K_{ABC})$. This is equivalent to $K_\Delta|\psi\rangle \propto |\psi\rangle$ in Eq. (1). Note that the left equation in Eq. (1), $K_\Delta \propto I$, does not follow from $K_\Delta|\psi\rangle \propto |\psi\rangle$ and the critical point condition in general, but does follow under certain assumptions that will be explained later in this section.

More generally, the result can be extended to the ground state on a finite circle and the thermal state on an infinite line. In both cases, the entanglement entropy and the entanglement Hamiltonian are known [7, 14], so the proof strategy still works. The difference is to replace the cross-ratio η with the effective cross-ratio η_{eff} where $\eta_{\text{eff}}^L = \frac{\sin(\pi x_{12}/L)\sin(\pi x_{34}/L)}{\sin(\pi x_{13}/L)\sin(\pi x_{24}/L)}$ for the ground state on a circle of length L and $\eta_{\text{eff}}^\beta = \frac{\sinh(\pi x_{12}/\beta)\sinh(\pi x_{34}/\beta)}{\sinh(\pi x_{13}/\beta)\sinh(\pi x_{24}/\beta)}$ for the thermal state on an infinite line of inverse temperature β .

We now discuss the subtle relation between the operator equation $K_\Delta = \frac{c}{3}h(\eta)$ and the vector equation $K_\Delta|\psi\rangle = \frac{c}{3}h(\eta)|\psi\rangle$. We first present an argument that shows their equivalence for quantum field theories, then discuss the difference in their approximate versions. It is clear that the operator equation implies the vector equation and typically the other way does not hold for finite dimensional Hilbert spaces. One extreme example for finite dimensional Hilbert spaces is that $K_X = -\log \rho_X$ could have singularities when ρ_X has zero eigenvalues, while $K_X|\psi\rangle$ is still well-defined with continuity, because $\lim_{\lambda \rightarrow 0} \lambda \log \lambda = 0$. On the other hand, for quantum field theories, due to the Reeh-Schlieder theorem [15], $|\psi\rangle \in \mathcal{H}_{ABCD}$ is cyclic, which means $O_D|\psi\rangle$ is dense in \mathcal{H}_{ABC} for O_D supported on D . Because K_Δ is only supported on \mathcal{H}_{ABC} , K_Δ and O_D commutes, and we have $K_\Delta O_D|\psi\rangle = \frac{c}{3}h(\eta)O_D|\psi\rangle$. Since $O_D|\psi\rangle$ is dense, this implies the operator equation $K_\Delta = \frac{c}{3}h(\eta)$.

In the approximate case, one might hope that $K_\Delta \approx \frac{c}{3}h(\eta)$ in the operator norm and $K_\Delta|\psi\rangle \approx \frac{c}{3}h(\eta)|\psi\rangle$ in the vector norm. Numerically, we observe that the approximate operator equation does not hold, while the approximate vector equation holds. This suggests that the vector equation is more valid because it is stable against perturbation. Nevertheless, we suspect that the operator equation remains stable under a different norm which requires further investigation.

Analytic implications— In the last section, we established that $K_\Delta = \frac{c}{3}h(\eta)$ for any consecutive intervals A, B, C . In this section, we apply this relation to intervals with integer-valued endpoints which can be associated with a lattice model. The benefit of having a lattice model is that it allows for concrete numerical ver-

ifications. We demonstrate that several quantities can be expressed as a sum of local operators. First, we prove that the EH of an interval can be expressed as a sum of 1-site and 2-site EHs from Eq. (1). This implies that the reduced density matrix on an arbitrary interval can be reconstructed from the 2-site reduced density matrix. Then, we define 6 operators generated by 1-site and 2-site EHs. When the state is a CFT ground state, these 6 operators correspond to the 6 global conformal generators. We then show that from Eq. (1) alone, without assuming the state is a CFT ground state, these 6 operators have the expected scaling properties under real-space RG. Some of the results in this section can be generalized to the ground state on a finite circle and the thermal state on an infinite line. In particular, we will numerically compute the Hamiltonian H and the momentum operator P on a finite circle in the next section.

We first introduce the notation. To simplify the presentation, we define the reduced EH as $\tilde{K}_X := K_X - \langle\psi|K_X|\psi\rangle$, which is the EH shifted by a constant so that $\langle\psi|\tilde{K}_X|\psi\rangle = 0$. This removes the constant term in Eq. (6), which implies that $\tilde{K}_\Delta = 0$. The reduced EH of an interval $[a, b]$ is denoted as $\tilde{K}_{[a,b]}$. In the following discussion, we only consider intervals with $a, b \in \mathbb{Z}$, so that they can be associated with a lattice model. The corresponding lattice model regards each interval of length 1, $[a, a + 1]$, as a single site. Therefore, the interval $[a, b]$ corresponds to $b - a$ sites. From now on, we refer to the reduced EH simply as EH.

We now show that any EH of an interval can be written as a sum of 1-site and 2-site EHs, using Eq. (1) recursively. We begin with the example of a 3-site EH. Take $A = [0, 1], B = [1, 2], C = [2, 3]$. The equivalent form of Eq. (1) $K_\Delta = 0$ implies

$$\tilde{K}_{[0,2]} + \tilde{K}_{[1,3]} - \frac{1}{4}\tilde{K}_{[0,1]} - \frac{1}{4}\tilde{K}_{[2,3]} - \frac{3}{4}\tilde{K}_{[1,2]} - \frac{3}{4}\tilde{K}_{[0,3]} = 0. \quad (10)$$

Therefore,

$$\tilde{K}_{[0,3]} = -\frac{1}{3}\tilde{K}_{[0,1]} + \frac{4}{3}\tilde{K}_{[0,2]} - \tilde{K}_{[1,2]} + \frac{4}{3}\tilde{K}_{[1,3]} - \frac{1}{3}\tilde{K}_{[2,3]}. \quad (11)$$

Similarly, for a 4-site EH, take $A = [0, 1], B = [1, 2], C = [2, 4]$, and we have

$$\begin{aligned} \tilde{K}_{[0,4]} &= -\frac{1}{2}\tilde{K}_{[0,1]} + \frac{3}{2}\tilde{K}_{[0,2]} - \tilde{K}_{[1,2]} + \frac{3}{2}\tilde{K}_{[1,4]} - \frac{1}{2}\tilde{K}_{[2,4]} \\ &= -\frac{1}{2}\tilde{K}_{[0,1]} + \frac{3}{2}\tilde{K}_{[0,2]} - \frac{3}{2}\tilde{K}_{[1,2]} + 2\tilde{K}_{[1,3]} \\ &\quad - \frac{3}{2}\tilde{K}_{[2,3]} + \frac{3}{2}\tilde{K}_{[2,4]} - \frac{1}{2}\tilde{K}_{[3,4]}. \end{aligned} \quad (12)$$

More generally, for an n -site EH, take $A = [0, 1], B = [1, 2], C = [2, n]$, and we have

$$\tilde{K}_{[0,n]} = -\frac{n-2}{n}\tilde{K}_{[0,1]} + \frac{2(n-1)}{n}\tilde{K}_{[0,2]} - \tilde{K}_{[1,2]}$$

$$+ \frac{2(n-1)}{n} \tilde{K}_{[1,n]} - \frac{n-2}{n} \tilde{K}_{[2,n]}. \quad (13)$$

By recursively expanding $\tilde{K}_{[1,n]}$ and $\tilde{K}_{[2,n]}$, we obtain

$$\tilde{K}_{[0,n]} = \sum_{j=-\infty}^{\infty} f_2(j+1) \tilde{K}_{[j,j+2]} + f_1(j + \frac{1}{2}) \tilde{K}_{[j,j+1]} \quad (14)$$

where $f_2(x) = \frac{2x(n-x)}{n} 1_{[0,n]}$, $f_1(x) = \frac{-2x(n-x) + \frac{3}{2}}{n} 1_{[0,n]}$, and $1_{[0,n]}$ is the indicator function. Therefore, any EH can be written as a sum of 1-site and 2-site EHs, which means the reduced density matrix on arbitrary regions can be reconstructed from the 2-site reduced density matrix. This could be viewed as a solution to the quantum marginal problem for CFTs where the Petz recovery map does not apply.

We note that the decomposition of EH into a sum of 1-site and 2-site EHs is similar to Eq. (6) in field theory, where EH is a sum of local terms $T_{00}(x)$. We also remark that there are different ways to decompose $\tilde{K}_{[0,n]}$, yet all of them lead to the same expression. This nontrivial property implies certain consistency relations between $\tilde{K}_{\Delta} = 0$ across different choices of A, B, C .

We now study the 6 global conformal generators $H, P, D, M_{10}, C_0, C_1$ which are the Hamiltonian, momentum, dilatation, boost, and special conformal generators. We first find their corresponding expressions for CFT ground states when Eq. (6) applies. Because $H = \int_{-\infty}^{\infty} dx T_{00}(x)$, $M_{10} = \int_{-\infty}^{\infty} dx x T_{00}(x)$, $C_0 = \int_{-\infty}^{\infty} dx x^2 T_{00}(x)$, applying Eq. (6), we have

$$\begin{aligned} H &= \frac{1}{\pi} \sum_{j=-\infty}^{\infty} \left(\tilde{K}_{[j,j+2]} - \tilde{K}_{[j,j+1]} \right) \\ &= \frac{1}{\pi} \sum_{j=-\infty}^{\infty} \tilde{K}'_{[j,j+2]}, \end{aligned} \quad (15)$$

$$\begin{aligned} M_{10} &= \frac{1}{2\pi} \sum_{j=-\infty}^{\infty} \left((2j+2) \tilde{K}_{[j,j+2]} - (2j+1) \tilde{K}_{[j,j+1]} \right) \\ &= \frac{1}{\pi} \sum_{j=-\infty}^{\infty} (j+1) \tilde{K}'_{[j,j+2]}, \end{aligned} \quad (16)$$

$$\begin{aligned} C_0 &= \frac{1}{\pi} \sum_{j=-\infty}^{\infty} \left((j+1)^2 \tilde{K}_{[j,j+2]} - (j^2 + j + 1) \tilde{K}_{[j,j+1]} \right) \\ &= \frac{1}{\pi} \sum_{j=-\infty}^{\infty} \left((j+1)^2 \tilde{K}'_{[j,j+2]} - \frac{1}{2} \tilde{K}_{[j,j+1]} \right), \end{aligned} \quad (17)$$

where $\tilde{K}'_{[j,j+2]} = \tilde{K}_{[j,j+2]} - \frac{1}{2} \tilde{K}_{[j,j+1]} - \frac{1}{2} \tilde{K}_{[j+1,j+2]}$ is introduced to simplify the equations. Because $P = \mathbf{i}[M_{10}, H]$, $D = \frac{1}{2}[C_0, H]$, $C_1 = \mathbf{i}[C_0, M_{10}]$, we have

$$P = \frac{\mathbf{i}}{\pi^2} \sum_{j=-\infty}^{\infty} \left[\tilde{K}'_{[j+1,j+3]}, \tilde{K}'_{[j,j+2]} \right], \quad (18)$$

$$\begin{aligned} D &= \frac{\mathbf{i}}{\pi^2} \sum_{j=-\infty}^{\infty} \left((j + \frac{3}{2}) \left[\tilde{K}'_{[j+1,j+3]}, \tilde{K}'_{[j,j+2]} \right] \right. \\ &\quad \left. - \frac{1}{4} \left[\tilde{K}_{[j,j+1]}, \tilde{K}'_{[j,j+2]} \right] \right. \\ &\quad \left. - \frac{1}{4} \left[\tilde{K}_{[j+1,j+2]}, \tilde{K}'_{[j,j+2]} \right] \right), \end{aligned} \quad (19)$$

$$\begin{aligned} C_1 &= \frac{\mathbf{i}}{\pi^2} \sum_{j=-\infty}^{\infty} \left((j+1)(j+2) \left[\tilde{K}'_{[j+1,j+3]}, \tilde{K}'_{[j,j+2]} \right] \right. \\ &\quad \left. - \frac{j+1}{2} \left[\tilde{K}_{[j,j+1]}, \tilde{K}'_{[j,j+2]} \right] \right. \\ &\quad \left. - \frac{j+1}{2} \left[\tilde{K}_{[j+1,j+2]}, \tilde{K}'_{[j,j+2]} \right] \right). \end{aligned} \quad (20)$$

This constructs the 6 global conformal generators from 1-site and 2-site EHs.

We make two comments on the expression for P . First, a similar expression was considered in [16, Sec II.C]. The idea is to define the momentum density $p_j = \mathbf{i}[h_j, h_{j-1}]$ in terms of the Hamiltonian density h_j where $H = \sum h_j$. One challenge in implementing this idea in practice is that the Hamiltonian H is only equal to the CFT Hamiltonian H_{CFT} up to a multiplicative factor. Consequently, the momentum density p_j is determined only up to a multiplicative factor. In our work, we fix this multiplicative factor and provide a better theoretical understanding. Second, there is a no-go theorem that prevents expressing the momentum operator as a sum of local operators [17, Corollary 6.1] which seemingly contradicts our expression above. There are several ways to reconcile this apparent contradiction. One is to note that our expression holds exactly only for lattice models with an infinite local Hilbert space dimension, whereas the no-go theorem applies to models with a finite local Hilbert space dimension. Another way to reconcile this is to recognize that, for models with a finite local Hilbert space dimension, $e^{-\mathbf{i}P}$ is not precisely equal to the lattice translation operator. Instead, they are only approximately equal at low energies as we verify numerically below.

We further comment that there are additional commutation relations between the generators which are not utilized in this work, such as $[M_{10}, P] = -\mathbf{i}H$ and $[H, P] = 0$. In the context of field theories, this phenomenon where higher order commutator of EHs are related to linear combinations of EHs can be understood from the operator product expansion (OPE) of $T_{zz}(t, x)$. First, because EH is a sum of $T_{zz}(t=0, x)$ and $T_{\bar{z}\bar{z}}(t=0, x)$, the commutator of EHs is a sum of the commutators of $T_{zz}(t=0, x)$ and $T_{\bar{z}\bar{z}}(t=0, x)$. Second, the commutator of $T_{zz}(t=0, x)$ is generated by the singular part of the OPE of T_{zz} . Finally, the singular part of the OPE of T_{zz} is generated by T_{zz} and its descendent $\partial_z T_{zz}$. The second and the final part can be summarized into the following

expression [18, Equation (B23)]

$$\begin{aligned} [T_{zz}(0, x_1), T_{zz}(0, x_2)] &= \frac{\mathbf{i}\pi c}{6} \partial_{x_1}^3 \delta(x_1 - x_2) \\ &+ 4\pi \mathbf{i} T_{zz}(0, x_2) \partial_{x_1} \delta(x_1 - x_2) \\ &- 2\pi \mathbf{i} \partial_z T_{zz}(0, x_2) \delta(x_1 - x_2). \end{aligned} \quad (21)$$

We leave these further relations between the higher order commutators of EHs and the linear combinations of EHs for future study.

Having defined the 6 conformal generators using 1-site and 2-site EHs, we now show that they have the expected scaling from real-space RG. We first study the case of the Hamiltonian H . To perform real-space RG, we consider a new system which blocks 2 sites in the original system into 1 site. We then compare the two reconstructed Hamiltonians using Eq. (15), which are

$$H_1 = \frac{1}{\pi} \sum_{j=-\infty}^{\infty} \tilde{K}_{[j,j+2]} - \tilde{K}_{[j,j+1]} \quad (22)$$

$$H_2 = \frac{1}{\pi} \sum_{j=-\infty}^{\infty} \tilde{K}_{[2j,2j+4]} - \tilde{K}_{[2j,2j+2]}. \quad (23)$$

Note that the state we used for the reconstructions is the same. The only difference is the size of the block. By expanding the 4-site EH as a sum of 1-site and 2-site EH using Eq. (12), we have $H_2 = 2H_1$. Similarly, one can define P_2 and show that $P_2 = 2P_1$, $D_2 = D_1$, $(M_{10})_2 = (M_{10})_1$, $(C_0)_2 = \frac{1}{2}(C_0)_1$, and $(C_1)_2 = \frac{1}{2}(C_1)_1$. These are precisely the scalings of the generators for CFT under the transformation $x \rightarrow x/2$, $t \rightarrow t/2$.

It is perhaps not surprising that the scaling property holds because the construction is motivated by the field theories. However, what is surprising is that the derivation of the scaling property only uses the condition (1), which is independent from the field theory description of CFTs. This observation supports the conjecture that states satisfying Eq. (1) are the CFT ground states.

Numerical tests— We now move on to numerics and verify that Eqs. (1), (3), (15) and (18) hold approximately for critical lattice models. First, we test the validity of the main Eqs. (1) and (3) on small sizes of four different critical lattice models and on large sizes of free fermions. We find that these equations hold approximately for all the models we consider and the error decreases as the size increases. Then, we test the reconstruction of the Hamiltonian and momentum operator Eqs. (15) and (18) on small sizes of the four models.

The critical lattice models we consider are the critical transverse field Ising model, critical three-state Potts model, XX model, and Heisenberg model defined as:

$$H_{\text{Ising}} = \sum_i -Z_i - X_i X_{i+1} \quad (24)$$

L	Error in Eq. (1)			Error in Eq. (3)		
	4	8	12	4	8	12
Ising Model	0.0282	0.0090	0.0057	0.0288	0.0090	0.0057
Potts Model	0.0422			0.0434		
XX Model	0	0.0399	0.0120	0.0486	0.0416	0.0125
Heisenberg	0	0.0562	0.0279	0.0566	0.0583	0.0286

TABLE I. The error in Eq. (1) $|K_{\Delta}|\psi\rangle - \langle\psi|K_{\Delta}|\psi\rangle|\psi\rangle$ and the error in Eq. (3) $|K_{\Delta}|\psi\rangle - \frac{\epsilon}{3}h(\eta)|\psi\rangle$ for ground states on circles with circumferences $L = 4, 8, 12$.

$$H_{\text{Potts}} = \sum_i -Z_i - Z_i^\dagger - \mathcal{X}_i \mathcal{X}_{i+1}^\dagger - \mathcal{X}_i^\dagger \mathcal{X}_{i+1} \quad (25)$$

$$H_{\text{XX}} = \sum_i X_i X_{i+1} + Y_i Y_{i+1} \quad (26)$$

$$H_{\text{Heisenberg}} = \sum_i X_i X_{i+1} + Y_i Y_{i+1} + Z_i Z_{i+1} \quad (27)$$

where X, Y, Z are the Pauli matrices and \mathcal{X}, \mathcal{Z} are the qutrit Pauli matrices

$$\mathcal{X} = \begin{pmatrix} 0 & 1 & 0 \\ 0 & 0 & 1 \\ 1 & 0 & 0 \end{pmatrix}, \quad \mathcal{Z} = \begin{pmatrix} 1 & 0 & 0 \\ 0 & \omega & 0 \\ 0 & 0 & \omega^2 \end{pmatrix}, \quad \omega = e^{2\pi\mathbf{i}/3} \quad (28)$$

Table I lists the errors associated with Eqs. (1) and (3). The error in Eq. (1) is defined as the norm of the component in $K_{\Delta}|\psi\rangle$ orthogonal to $|\psi\rangle$, $|K_{\Delta}|\psi\rangle - \langle\psi|K_{\Delta}|\psi\rangle|\psi\rangle$, which is also the standard deviation of K_{Δ} , $\sqrt{\langle K_{\Delta}^2 \rangle - \langle K_{\Delta} \rangle^2}$. The error in Eq. (3) is defined as the norm $|K_{\Delta}|\psi\rangle - \frac{\epsilon}{3}h(\eta)|\psi\rangle$. We computed these errors for ground states on circles with circumferences $L = 4, 8, 12$, where (A, B, C) have lengths $(1, 1, 1)$, $(2, 2, 2)$, and $(3, 3, 3)$, respectively. In all cases, $\eta = 1/2$. We observe that except for the accidental case where the XX model and Heisenberg model with circumference 4 have 0 errors, the error decreases as the system size increases. This result is consistent with the intuition that the lattice model approximates the CFT better in the IR as the system size increases.

Figure 2 shows the error in Eq. (1) for free fermions across various system sizes. We again observe that the error decreases as the system size increases which roughly scales as $1/L^2$. Simulating free fermions on a large system size is feasible due to their lower complexity [19, 20].

We now test the reconstructed Hamiltonian and momentum on a circle in Eqs. (3) and (4) where

$$H_{\text{rec}} = \frac{\sin(2\pi/L)}{2L \sin^2(\pi/L)} \sum_{j=0}^{L-1} \tilde{K}_{[j,j+2]} - \tilde{K}_{[j,j+1]} \quad (29)$$

$$P_{\text{rec}} = \frac{\mathbf{i}}{\pi^2} \sum_{j=0}^{L-1} [\tilde{K}'_{[j+1,j+3]}, \tilde{K}'_{[j,j+2]}]. \quad (30)$$

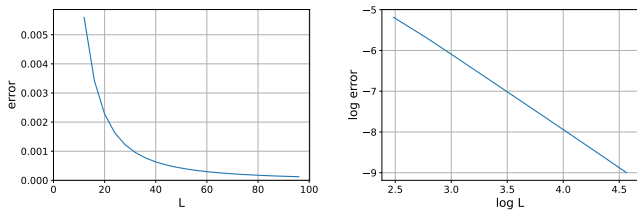


FIG. 2. The error in Eq. (1) $\left| K_\Delta |\psi\rangle - \langle \psi | K_\Delta |\psi\rangle |\psi\rangle \right|$ for the ground state of the critical free fermions. The circle is partitioned into four equal sized intervals, where the lengths of A, B, C are $L/4$ and has cross ratio $\eta = 1/2$. The error roughly scales as $1/L^2$.

The factor $\frac{\sin(2\pi/L)}{2L \sin^2(\pi/L)}$ in H_{rec} comes from the coefficient obtained when expressing EH as an integral of $T_{00}(x)$. On the other hand, the factor $\frac{i}{\pi^2}$ in P_{rec} is based solely on the understanding at the infinite-size limit in Eq. (18). Despite this, as we will see, the reconstructed Hamiltonian and momentum agree excellently.

Before presenting the result, we first remark that the field theory Hamiltonian and momentum satisfy

$$H_{CFT} |\Delta, s\rangle = \frac{2\pi}{L} \left(\Delta - \frac{c}{12} \right) |\Delta, s\rangle \quad (31)$$

$$P_{CFT} |\Delta, s\rangle = \frac{2\pi}{L} s |\Delta, s\rangle, \quad (32)$$

where $|\Delta, s\rangle$ is the image under the state-operator correspondence of a scaling operator of dimension Δ and spin s . We emphasize that H_{rec} is equal to H_{CFT} up to a constant shift so that H_{rec} has ground state energy 0, i.e. $H_{rec} = H_{CFT} - E_0$.³ In particular, the multiplicative factor is fixed, meaning that the scaling dimensions Δ can be obtained without the rescaling required if one directly uses the spectrum of an arbitrary critical Hamiltonian.

Figure 3 compares the spectra of the original Hamiltonian to the spectrum of the reconstructed Hamiltonian at low energy. The reconstructed Hamiltonian H_{rec} is rescaled by $\frac{L}{2\pi}$ and the original Hamiltonian is rescaled to fit H_{rec} . We observe the spectra have excellent agreement even at the small system size where $L = 4$.

Figure 4 compares the spectrum of $i \log T$ to the spectrum of the reconstructed momentum at low energy, where T is the translation operator by 1 site. We test if $T \approx e^{-iP_{rec}}$. Again both spectra are rescaled by $\frac{L}{2\pi}$ and we expect both to take integer values. We observe

³ The constant $-\frac{2\pi}{L} \frac{c}{12}$ can be recovered by using the EHs of the ground state on an infinite system instead of the EHs of the length L finite system, which we have tested for critical free fermions. However, we do not discuss this aspect further because it is generally not possible to know the EHs on an infinite system directly.

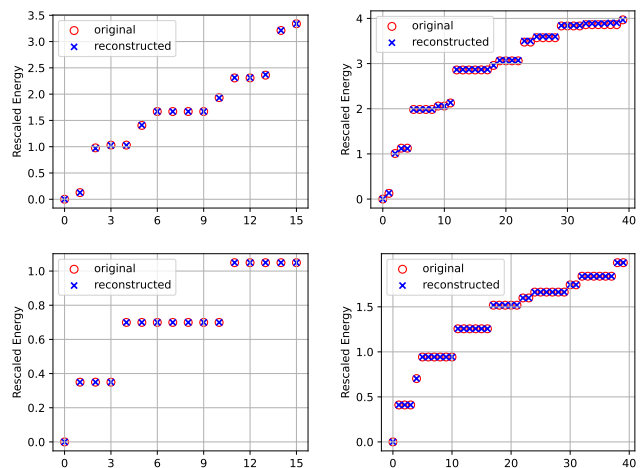


FIG. 3. Spectra of the original Hamiltonian and the reconstructed Hamiltonian, where the states are ordered by energy along the X-axis. Top left: Ising model with $L = 4$. Top right: Lowest 40 eigenvalues for Ising model with $L = 12$. Bottom left: Heisenberg model with $L = 4$. Bottom right: Lowest 40 eigenvalues for Heisenberg model with $L = 12$.

the spectra agree at low energy and the agreement improves as the system size increases.

We provide three technical comments on this test. First, we note that in lattice models, it is not generally true that $T = e^{-iP_{CFT}}$, for example, in the Heisenberg and XX models. This is because $i \log T$ may have a constant shift s_0 , where $i \log T |\psi\rangle = (s_0 + \frac{2\pi}{L} s) |\psi\rangle$. As an example, if we instead define the transverse field Ising model as $H_{\text{Ising}} = \sum_i -Z_i + X_i X_{i+1}$, then the new ground state is obtained by applying Z on the even sites of the usual ground state. This results with a shift $s_0 = \pi$. Sometimes this shift cannot be removed easily due to anomaly [21]. This is why we did not show the reconstruction in the case of Heisenberg and XX models for simplicity. Next, we remark on two surprising properties of P_{rec} . One is that $\frac{L}{2\pi} P_{rec}$ is close to taking integer values at low energy. The other is that it is often the case that $-\pi \leq P_{rec} \leq \pi$. Both properties are expected when knowing $T \approx e^{-iP_{rec}}$. However, from Eq. (30) alone, it is unclear why this happens; we leave this for future research. Finally, although we lack a full analytic understanding of the factor $\frac{i}{\pi^2}$ in P_{rec} , it works well numerically. The precise nature of this factor on a finite system, and whether this is a correct choice or merely a coincidence, is left for further exploration.

Further directions— The further directions are sorted based on some subjective measure of attractiveness.

(a) We show that CFT ground states satisfy the condition in Eq. (1). Motivated by entanglement bootstrap, we ask whether the converse is also true, i.e. if a state satisfying the condition can be interpreted as a CFT ground state. Additionally, we would like the statement to be

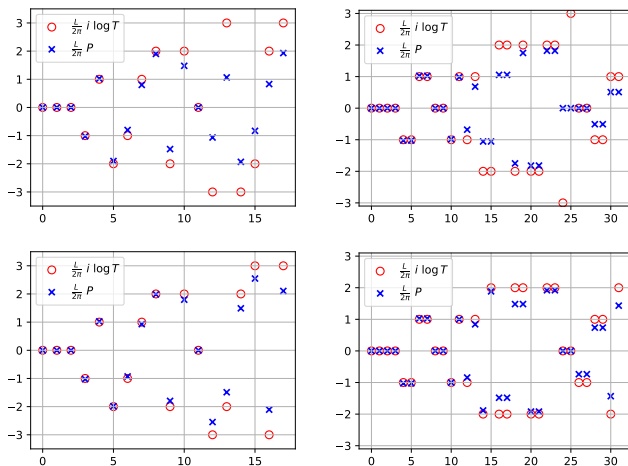


FIG. 4. Spectra of $i \log T$ and the reconstructed momentum operator P , where T is the translation operator by 1 site. The states are ordered by energy along the X-axis. In the infinite-size limit, this order corresponds to the order of the scaling dimension of the corresponding operator from the state-operator correspondence. For the small system sizes shown here, these orders are not yet the same. This is why the order changes in the figure when the system size changes. Top left: Ising model with $L = 8$. Bottom left: Ising model with $L = 12$. Top right: Potts model with $L = 6$. Bottom right: Potts model with $L = 8$.

robust, useful even when the state only satisfies the condition approximately.

(b) We proposed various formulas that hold exactly when the state is a CFT ground state. However, for the ground state of critical lattice models, the formula only holds approximately. What is the convergence behavior and the finite size scaling?

(c) Relatedly, one may wonder if we allow combinations of not only 1-site and 2-site EH but also 3-site EH, which combination has the best approximation to the Hamiltonian and the momentum. Furthermore, what if we include EH on larger sites? Could this lead to a sequence of reconstructions that converges to the actual operator? Finding a good approximation is crucial for obtaining a better estimation of the OPE based on the method discussed in [22].

(d) Can we reproduce the key results in CFT directly using quantum information? For example, can we show that all nontrivial states must have $c \geq \frac{1}{2}$? Can we show the ground state energy is $-\frac{2\pi}{L} \frac{c}{12}$ on a circle with circumference L ? Can we show that the reconstructed momentum operator should be approximately integer valued at low energy and has a norm roughly below π ?

(e) The appearance of $h(\eta)$ in Eq. (3) suggests that η can be interpreted as a probability. Could we find a physical meaning for this observation?

(f) We provide an information theoretic criterion for CFT ground state. Can we transform this criterion into

an algorithm that searches for CFTs by screening states that satisfy Eq. (1)? We believe the answer is yes and plan to explore this aspect in an upcoming paper.

(g) We provide an entropy criterion that appears to describe ground states for 1+1D unitary CFTs. We suspect a similar formula exists for 1+1D chiral CFTs and d+1D CFTs.

(h) We show that CFT ground states are critical points of the function S_Δ , with a value proportional to the central charge. What is its relation to the Zamolodchikov c -function [23] and the entropic c -function [24]? For example, it is known that the second and third-order expansion of the Zamolodchikov c -function near the CFT point contains the CFT data, including the scaling dimensions and the OPEs. Does the same hold for the entropy function we proposed?

(i) We showed that 1+1D phases at RG fixed points with Lorentz symmetry satisfy Eq. (1). What happens to other RG fixed points without Lorentz symmetry, such as those with dynamical critical exponent $z \neq 1$. In the case of free fermion models with $z \in \mathbb{Z}^{>0}$, the formula continues to hold. When z is even, the ground state is simply a product state, and when z is odd, the ground state is same as the ground state for $z = 1$, which is a CFT.

Acknowledgments— We thank Isaac Kim and Hao-Chung Cheng for suggesting a simple proof to compute the first-order derivative of entanglement entropy in Eq. (8). We thank Meng Cheng and Yijian Zhou for clarifying why in general $T \neq e^{-iP}$. We thank Bowen Shi and Daniel Ranard for helpful discussions. This work was supported in part by funds provided by the U.S. Department of Energy (D.O.E.) under the cooperative research agreement DE-SC0009919, and by the Simons Collaboration on Ultra-Quantum Matter, which is a grant from the Simons Foundation (652264, JM). TCL would like to thank the assistance of ChatGPT in improving parts of the paper for clarity, including this sentence.

-
- [1] A. Kitaev and J. Preskill, “Topological entanglement entropy,” *Physical review letters* **96** (2006), no. 11 110404.
 - [2] M. Levin and X.-G. Wen, “Detecting topological order in a ground state wave function,” *Physical review letters* **96** (2006), no. 11 110405.
 - [3] H. Li and F. D. M. Haldane, “Entanglement spectrum as a generalization of entanglement entropy: Identification of topological order in non-abelian fractional quantum hall effect states,” *Physical review letters* **101** (2008), no. 1 010504.
 - [4] I. H. Kim, B. Shi, K. Kato, and V. V. Albert, “Chiral central charge from a single bulk wave function,” *Physical Review Letters* **128** (2022), no. 17 176402.
 - [5] C. Holzhey, F. Larsen, and F. Wilczek, “Geometric and

- renormalized entropy in conformal field theory,” *Nuclear physics b* **424** (1994), no. 3 443–467.
- [6] P. Calabrese and J. Cardy, “Entanglement entropy and quantum field theory,” *Journal of statistical mechanics: theory and experiment* **2004** (2004), no. 06 P06002.
- [7] P. Calabrese and J. Cardy, “Entanglement entropy and conformal field theory,” *Journal of physics a: mathematical and theoretical* **42** (2009), no. 50 504005.
- [8] B. Shi, K. Kato, and I. H. Kim, “Fusion rules from entanglement,” *Annals of Physics* **418** (2020) 168164.
- [9] B. Shi and I. H. Kim, “Entanglement bootstrap approach for gapped domain walls,” *Physical Review B* **103** (2021), no. 11 115150.
- [10] J.-L. Huang, J. McGreevy, and B. Shi, “Knots and entanglement,” *arXiv preprint arXiv:2112.08398* (2021).
- [11] E. H. Lieb and M. B. Ruskai, “Proof of the strong subadditivity of quantum-mechanical entropy,” *Les rencontres physiciens-mathématiciens de Strasbourg-RCP25* **19** (1973) 36–55.
- [12] M. A. Nielsen and I. Chuang, “Quantum computation and quantum information,” 2002.
- [13] D. Perez-Garcia, F. Verstraete, M. M. Wolf, and J. I. Cirac, “Matrix product state representations,” *arXiv preprint quant-ph/0608197* (2006).
- [14] J. Cardy and E. Tonni, “Entanglement hamiltonians in two-dimensional conformal field theory,” *Journal of Statistical Mechanics: Theory and Experiment* **2016** (2016), no. 12 123103.
- [15] H. Reeh and S. Schlieder, “Bemerkungen zur unitäräquivalenz von lorentzinvarianten feldern,” *Il Nuovo Cimento (1955-1965)* **22** (1961), no. 5 1051–1068.
- [16] A. Milsted and G. Vidal, “Extraction of conformal data in critical quantum spin chains using the Koo-Saleur formula,” *Physical Review B* **96** (2017), no. 24 245105.
- [17] D. Ranard, M. Walter, and F. Witteveen, “A converse to Lieb–Robinson bounds in one dimension using index theory,” in *Annales Henri Poincaré*, vol. 23, pp. 3905–3979, Springer, 2022.
- [18] Y. Zou, B. Shi, J. Sorce, I. T. Lim, and I. H. Kim, “Modular Commutators in Conformal Field Theory,” *Physical Review Letters* **129** (2022), no. 26 260402.
- [19] I. Peschel and V. Eisler, “Reduced density matrices and entanglement entropy in free lattice models,” *Journal of physics a: mathematical and theoretical* **42** (2009), no. 50 504003.
- [20] M. Fagotti and P. Calabrese, “Entanglement entropy of two disjoint blocks in XY chains,” *Journal of Statistical Mechanics: Theory and Experiment* **2010** (2010), no. 04 P04016.
- [21] M. Cheng and N. Seiberg, “Lieb-Schultz-Mattis, Luttinger, and ’t Hooft–anomaly matching in lattice systems,” *arXiv preprint arXiv:2211.12543* (2022).
- [22] Y. Zou, A. Milsted, and G. Vidal, “Conformal fields and operator product expansion in critical quantum spin chains,” *Physical Review Letters* **124** (2020), no. 4 040604.
- [23] A. B. Zamolodchikov, “Irreversibility of the Flux of the Renormalization Group in a 2D Field Theory,” *JETP lett* **43** (1986), no. 12 730–732.
- [24] H. Casini and M. Huerta, “A c-theorem for entanglement entropy,” *Journal of Physics A: Mathematical and Theoretical* **40** (2007), no. 25 7031.
- [25] D. Sutter, M. Berta, and M. Tomamichel, “Multivariate trace inequalities,” *Communications in Mathematical Physics* **352** (2017) 37–58.

Supplemental Material

Proof of Eq. (8)

Let $|\psi\rangle \in \mathcal{H}_A \otimes \mathcal{H}_B$ be a pure state. We now show the first order derivative of entanglement entropy $S_A(|\psi\rangle)$ claimed in Eq. (8). Because $d\rho_A = \text{Tr}_B(|\psi\rangle\langle d\psi|) + \text{Tr}_B(|d\psi\rangle\langle\psi|)$, it is sufficient to show

$$dS(\rho_A) = \text{Tr}_A((-\log \rho_A)d\rho_A). \quad (33)$$

Using product rule in calculus,

$$dS(\rho) = d\text{Tr}((-\log \rho)\rho) = \text{Tr}((-\log \rho)d\rho) - \text{Tr}(\rho d(\log \rho)). \quad (34)$$

We suffice to show the second term on the RHS is 0. This is done by showing

$$\text{Tr}(\rho d(\log \rho)) = \text{Tr}(d\rho) \quad (35)$$

where $\text{Tr}(d\rho) = d\text{Tr}(\rho) = 0$.

Because ρ is hermitian, we can write $\rho = e^M$. Equivalently, we need to show

$$\text{Tr}(e^M dM) = \text{Tr}(de^M). \quad (36)$$

This is obtained by an equation from the perturbation theory of path integrals

$$de^M = \int_0^1 dt e^{tM} dM e^{(1-t)M}. \quad (37)$$

We sketch the proof of the final equation:

$$de^M = \lim_{n \rightarrow \infty} d \prod_{i=1}^n e^{M/n} \quad (38)$$

$$= \lim_{n \rightarrow \infty} \sum_{i=1}^n e^{\frac{i-1}{n}M} (de^{M/n}) e^{\frac{n-i}{n}M} \quad (39)$$

$$= \lim_{n \rightarrow \infty} \sum_{i=1}^n e^{\frac{i-1}{n}M} (dM/n) e^{\frac{n-i}{n}M} \quad (40)$$

$$= \int_0^1 dt e^{tM} dM e^{(1-t)M} \quad (41)$$

where the third equality uses $e^{M/n} = I + M/n + O(1/n^2)$. The higher order term $O(1/n^2)$ converges to 0 as $n \rightarrow \infty$, because there are only n terms.

More directly, the key step Eq. (35) can also be obtained through the following equality [25, Lemma 3.4]

$$d \log \rho = \int_{-\infty}^{\infty} dt \beta_0(t) \rho^{-\frac{1+it}{2}} d\rho \rho^{-\frac{1-it}{2}} \quad (42)$$

where $\beta_0(t) = \frac{\pi}{2}(\cosh(\pi t) + 1)^{-1}$. When substituting $d \log \rho$ in Eq. (35), we obtain

$$\text{Tr}(\rho d(\log \rho)) = \int_{-\infty}^{\infty} dt \beta_0(t) \text{Tr}(d\rho) = \text{Tr}(d\rho) \quad (43)$$

using $\int_{-\infty}^{\infty} dt \beta_0(t) = 1$.